

Title No. 120-M56

Pertinent Surface Moisture of Concrete for Water Ingress Assessment

by Uwazuruonye Raphael Nnodim

This study clarifies the effects of moisture (expressed as percentage saturation degree of permeable pore voids, PSD) on water ingress properties of concrete and establishes a region where PSD does not affect the quantitative water absorption. Experimental measurements and finite element model (FEM) simulation results for ordinary portland cement (OPC) concretes preconditioned to equilibrium moisture formed plateaus between 21 and 58% PSD. Non-continuous finer capillary pores ($\phi 10$ nm [3.937×10^{-4} mil, thou] to $\phi 100$ nm [3.937×10^{-3} mil, thou]) constitute the empty pores within the plateau region before tests. Water sorptivity of OPC and slag cement concrete blocks at several degrees of surface moisture with internal moisture gradients validate the existence of the plateau within the PSD range. Measuring short-term water absorption within this plateau region eliminates the effects of initial surface moisture content on the measured properties and evaluates the continuity and connectivity of pores, which is the major indicator of the durability of concrete.

Keywords: durability; permeability; pore size distribution; transport properties.

INTRODUCTION

To what degree the cover zone of concrete resists moisture ingress is of paramount importance regarding durability of in-place concrete structures. Notwithstanding that there is no universally accepted quantifier for the general durability performance of concrete, the resistance to water ingress is arguably one of the greatest quantifiers in durability design and assessment of concrete structures against the ingress of deleterious materials as well as the initiation of concrete deterioration.¹ Regardless of the deterioration mechanism, water is needed to initiate almost all deterioration processes of concrete structures. Even the deteriorations that are inherent in the materials require water to begin.^{2,3}

Many durability test standards such as ASTM C1585,⁴ BS 1881 Part 207,⁵ and JSCE-G 582⁶ appropriately consider and evaluate the resistance to water ingress. Nonetheless, the quality of concrete in actual structures always differs from the design assumptions due to several effects resulting from concreting works; therefore, durability assessment of in-service concrete structures is important. The aforementioned test standards require drying concrete to a sufficiently steady weight and cannot be applied in-place. Resistance to water absorption has not been appropriately considered in the durability assessment of in-place concrete structures due to the ambiguous effects of moisture conditions. Moreover, covercrete, which is the channel for water infiltration, is also the most affected part by concreting works and is always different from the inner concrete.^{2,3,7,8}

Surface water absorption largely depends on the action of the capillary pores resulting from the pore diameters, pore

continuity/connectivity, tortuosity, and the degree of saturation. Furthermore, surface tension and viscosity, which are influenced by factors such as temperature, contribute a great deal to water permeability.⁹⁻¹¹ Short-term water penetration depth of concrete has an approximately linear relationship with the square root of immersion time.¹² However, this is for concrete that is dried to a steady weight, seemingly unable to experience further moisture loss. In the literature, it is difficult to find an appropriate initial saturation degree of the pore system for effective evaluation of resistance to water ingress of in-place concrete structures. Also, the coupled influence of capillary pore size distribution and saturation degree on moisture transfer has not been clarified.

In an investigation of the relationship among the permeation rate of water into concrete, mixture design, curing, and degree of drying, Sakai et al.¹³ propounded a simple equation to evaluate the water absorption in concrete. The equation assumed that water-binder ratio (w/b), curing, and degree of drying are dominant in water absorption. "As long as the amount of aggregate and mineral admixture are common, the sorptivity of concrete can be evaluated with the w/b , curing, and the degree of drying,"¹³ indicating an assumption of a linear relation. Parrott¹⁴ showed that sorptivity was linearly correlated with the amount of water loss by drying. Maruyama¹⁵ indicated the influence of dried C-S-H on water absorption. The C-S-H is said to shrink on drying and swells on water absorption and its amount may considerably affect sorptivity. This might not be far from the finding that during water uptake in relatively dry concrete, water redistributes to smaller pores and at the same time results in more internal swelling, which reduces the connectivity of the capillary pore system, thereby lowering the water uptake.¹² Using a nuclear magnetic resonance (NMR) test, Rucker-Gramm and Beddoe¹² revealed that water in gel pores decisively affected the transport of water in larger capillary pores.

Yokoyama et al.¹⁶ concluded that "water absorbency of concrete slabs is affected by the quantity of pores with diameters of approximately 10^{-7} m (100 nm [3.937×10^{-3} mil, thou]) and larger, while water content depends on the quantity of pores with diameters of approximately 10^{-8} m (10 nm [3.937×10^{-4} mil, thou]) and smaller." In a study of the relationship between the degree of drying and oxygen diffusion coefficient in hardened cement paste, results showed

ACI Materials Journal, V. 120, No. 5, September 2023.

MS No. M-2022-340.R1, doi: 10.14359/10.14359/51739018, received May 30, 2023, and reviewed under Institute publication policies. Copyright © 2023, American Concrete Institute. All rights reserved, including the making of copies unless permission is obtained from the copyright proprietors. Pertinent discussion including author's closure, if any, will be published ten months from this journal's date if the discussion is received within four months of the paper's print publication.

that between 15 and 45% relative humidity (RH), RH had no virtual effect on the oxygen diffusion coefficient (D_e -m²/s).¹⁷

Surface water absorption of in-place concrete is highly affected by the moisture condition before the measurement and specimen preconditioning influences sorptivity.^{18,19} Also, moisture content of in-place concrete is not uniform and always exhibits moisture gradient. The effect of moisture content on measured properties of concrete is the greatest challenge and limitation for all the in-place measurement devices^{2,3} such as Autoclam water/air permeability, double-chamber air permeability, electrical resistivity, surface water absorption test (SWAT), and so on. In this study, experimental investigations and numerical simulations are conducted and the surface moisture content is expressed as a percentage saturation degree of permeable pore voids (*PSD*), which is directly related to the volume of pore voids of the concrete.

RESEARCH SIGNIFICANCE

Many design methods evaluate the resistance of concrete to water ingress, but none have been effective for in-place concrete durability assessment due to the complex effects of moisture conditions. The effects of initial moisture contents on surface water absorption tests have been deeply researched without any proposal of the appropriate initial moisture contents for effective nondestructive assessment. This is the first detailed study clarifying the effects of moisture content on the resistance to surface water absorption for in-place concrete with a proposal of an appropriate initial surface moisture content that excludes the effect of moisture contents on the measured properties.

EXPERIMENTAL INVESTIGATION

Materials

Table 1 summarizes the different types of concretes used in this study, which were selected from among commonly used

concretes in Japan. Prismatic concrete specimens with 300 x 300 mm (11.811 x 11.811 in.) area and 150 mm (5.91 in.) thickness were prepared with ordinary portland cement (OPC) and slag cement (JIS Type B slag cement). The concrete specimens were prepared in two sets and were kept in a controlled room condition of 20°C (68°F) and 60% RH after curing until the absorption test preparation time. The first set is composed of three concrete types and is marked “‡” in Table 1, while the second set is composed of eight concrete types. The names of the specimens were coded to portray cement type, water-cement ratio (*w/c*), and type of curing. The curing conditions applied were 7D: 7 days sealed in mold, 10D: 10 days sealed in mold, and 10W: 1 day sealed in mold + 9 days in water after removing the mold. The procedure for fabricating the concrete test specimens in the laboratory followed the ASTM C192/C192M-02 standard practice. The concrete specimens were rodded with tamping rods while the molds were made of nonabsorbent smooth wooden form. All tests were conducted on the formwork finished surface of the concrete specimens.

Experimental methods

Preconditioning of moisture condition—To investigate the effects of saturation degree of pore voids on the resistance to water ingress, concrete cores of ϕ 100 mm (ϕ 3.94 in.) were taken along the 150 mm (5.91 in.) thickness at the age of 510 days from selected prismatic specimens (marked with “‡” in Table 1). The concrete needed a sufficient hydration degree to eliminate the possibility of microstructural change during preconditioning. The extracted cores were sliced, and two specimens were provided with 45 mm height and with the formwork-finished face (Fig. 1). To achieve moisture equilibrium inside the specimens at several saturation degrees of pore voids, the sliced specimens were preconditioned in a controlled humidity chamber (40°C [104°F] and

Table 1—Summary of concrete mixture proportions and curing conditions

Name of specimen	<i>w/c</i> , %	<i>s/a</i> , %	Mixture composition, kg/m ³				Admixtures		Curing
			Cement		Aggregate		Type*	Dosage [†]	
			Amount	Type	Fine	Coarse			
N40-7D‡	40	45	400	N	777	950	Ad-AE	1.1875	7D
N50-7D‡	50	47	320	N	841	948	Ad-AE	1.1985	7D
N60-7D‡	60	48.5	267	N	890	945	Ad-AE	1.3	7D
N40-10D	40	45	400	N	776	948	Ad-AE	1.1025	10D
N50-10D	50	47	320	N	840	947	Ad-AE	1.0025	10D
N60-10D	60	48.5	267	N	890	945	Ad-AE	1.0025	10D
BB50-10D	50	47	320	BB	831	937	Ad-AE	1.025	10D
N40-10W	40	45	400	N	776	948	Ad-AE	1.1025	10W
N50-10W	50	47	320	N	840	947	Ad-AE	1.0025	10W
N60-10W	60	48.5	267	N	890	945	Ad-AE	1.0025	10W
BB50-10W	50	47	320	BB	831	937	Ad-AE	1.025	10W

*Admixture types: Ad is water-reducing admixture; AE is air-entraining agent.

[†]Admixture dosage: percentage of admixtures to binder, weight-to-weight ratio.

[‡]Specimens from which cores were taken and preconditioned to equilibrium moisture distribution.

Note: N is ordinary portland cement, BB is slag cement (JIS Type B slag cement).

50% RH). The sealing materials and preconditioning steps have previously been established by the author²⁰ and can be summarized as follows:

- Saturating specimen by total immersion into water;
- Sealing the lateral sides with vinyl electric insulation tape;
- Drying the specimen to obtain the desired weight;
- Sealing the two faces of the specimen with a layer of polythene sheet;
- Returning the specimen to the controlled chamber to attain moisture equilibrium; and
- Storing the specimen in a different closed chamber to allow natural heat loss until the specimen is cooled down to approximately 20 to 25°C (68 to 77°F).

To investigate the sorptivity of concrete with moisture gradient such as in in-place concrete structures, eight kinds of prismatic specimens (without the “*” mark in Table 1) were provided without the preconditioning mentioned previously. During the placement of concrete, moisture sensors were embedded (in pairs, 10 mm apart) at 5, 10, 20, 30, and 50 mm (0.197, 0.394, 0.787, 1.181, and 1.969 in.) depths from the surface (Fig. 2) to monitor the moisture gradient

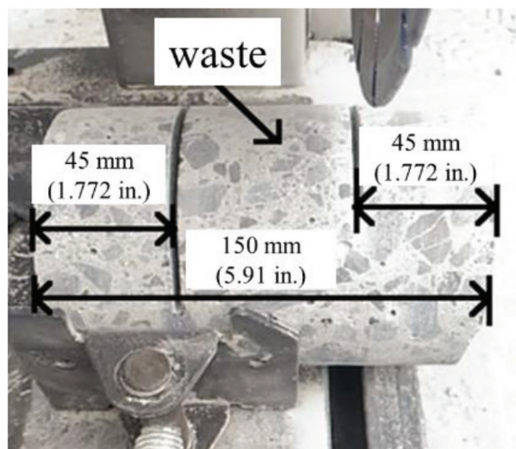


Fig. 1—Extraction of test samples used in preconditioned state.

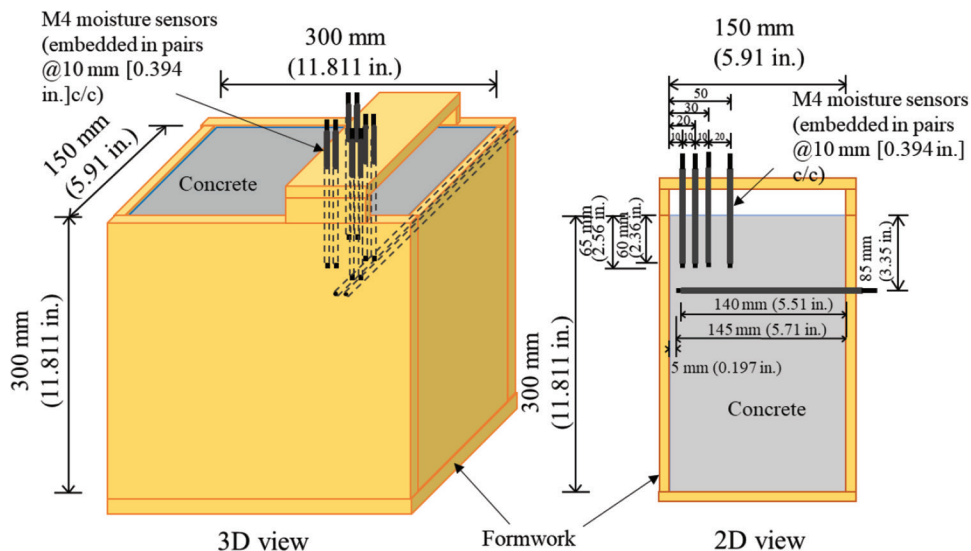


Fig. 2—Details of M4 moisture sensor locations in concrete blocks.

in the specimens by attaching a moisture meter (electric resistance type) to the sensors. A moisture sensor is a set of stainless direct-current-type (ϕ 4 mm [0.157 in.]) threaded rods that are embedded in pairs into the concrete to serve as the connecting electrodes to the moisture meter. It has an effective area of 4 mm diameter. To eliminate cracks due to the embedding of the moisture sensor in the very shallow concrete cover of 5 mm (0.197 in.), the moisture sensor for the 5 mm (0.197 in.) depth was embedded from the back (Fig. 2). The output of the moisture meter is expressed in moisture content or in “count values,” and the investigated relationship between the two outputs is shown in Fig. 3. It was previously confirmed that count values have an inverse relationship with electric resistance.²¹

To simulate many kinds of complicated internal moisture distribution and surface moisture contents for concrete in outdoor environments, at 90 days after the placement, the second set of concrete blocks were exposed to 60, 80, and 99% RH for a varying number of days. Three same specimens were provided for eight types of concretes shown in Table 1, and three specimens were exposed to different RH to obtain various kinds of moisture distribution. Measurements of surface moisture content and surface water absorption were conducted daily until 14 days from the exposure date using a surface moisture meter and SWAT device, respectively.

Measurement of percentage saturation degree of pore voids, PSD—PSD is measured using an electric resistance moisture meter by pressing the device onto the concrete surface; the results are expressed in count values. The surface moisture tester has an built-in hard-rubber-type sensor that measures when in contact with the surface of concrete. The advantages of this surface moisture meter over others is the ability to access both the pore water and the pore connectivity during measurements and the capacity to measure moisture content up to the depth of 5 mm from the surface.²² Figure 4 shows the relationship between PSD and count values measured with the surface moisture meter in a documented preliminary investigation.²⁰ The scatter plot showed a strong positive correlation between PSD and

moisture meter count values. The scatter plot was obtained from many kinds of concretes preconditioned to equilibrium internal moisture distribution.

Surface water absorption test procedure—For the samples preconditioned to equilibrium moisture distribution, two replicate samples (Fig. 5(a)) were tested by the SWAT to investigate the resistance to water ingress. Similarly, for the second set of concrete blocks without equilibrium moisture preconditioning, the average result from four measurement points (Fig. 5(b)) is used to obtain both the water sorptivity and count values.

The resistance against water absorption is expressed as the coefficient of surface water absorption, *CSWA* ($\text{mL}/\text{m}^2/\text{s}^{1/2}$). *CSWA* can be obtained from the slope of the approximate linear regression between water absorption amount and the square root of time. The author recently introduced the *CSWA* index and confirmed its correlations with the JSCE-G 582 sorptivity test results.⁸

SWAT (Appendix A) is a nondestructive device that evaluates the quality of covercrete in 10 minutes under natural water suction.^{23,24} SWAT is composed of a fully automatic

machine unit, an absorption cup (80 mm inner diameter and 100 mm outer diameter) with a calibrated cylindrical tube, water inlet and tap, a sensor, a framed vacuum pump for fixing or fixing clamp for small specimens, and a water container. The SWAT system does not require a constant water head throughout the testing time and the time for injecting water into the water absorption cup before test is 10 seconds. SWAT has been proven to be effective in detecting the influences of curing conditions, mixture proportions, and the adverse effects of microcracks in covercrete quality within 10 to 20 mm (0.394 to 0.787 in.), which is the most affected by concreting works.^{8,22-26} The rate of surface water absorption at 10 minutes (where the time for injecting water into the cup for measurement preparation is 10 seconds) measured by SWAT is termed p_{600} ($\text{mL}/\text{m}^2/\text{s}$) and the criterion for the conventional quality grading is shown in Table A1 of Appendix A. *CSWA* has a good correlation with p_{600} .⁸ Besides, good correlations have been demonstrated between p_{600} and long-term water penetration depth,²⁵ as well as the carbonation rate coefficient of concrete.²⁷

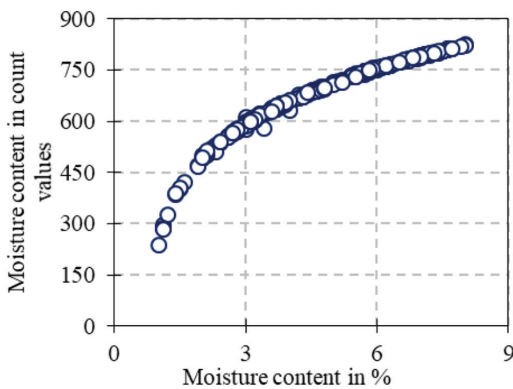


Fig. 3—Relationship between count values and percentage values of HI-800 moisture meter.

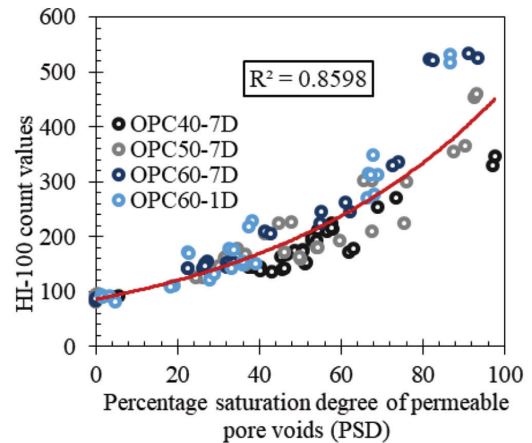


Fig. 4—Relationship between PSD and HI-100 moisture meter count values.

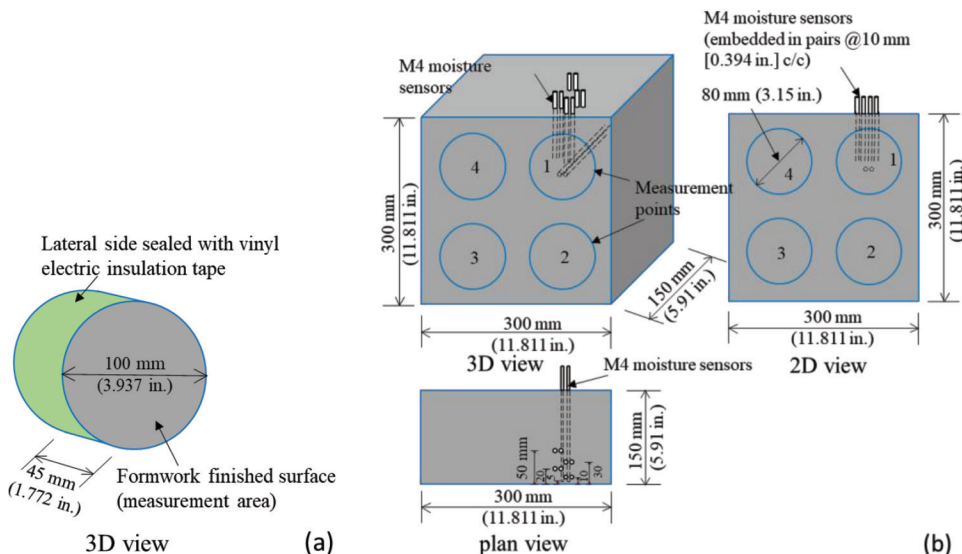


Fig. 5—Measurement of water sorptivity of concrete by SWAT device: (a) sample pre-conditioned to equilibrium moisture distribution; and (b) concrete block with internal moisture gradient.

NUMERICAL SIMULATION

Simulation tool—To investigate the effective pore diameter available for water transport at different percentage saturation degrees of pore voids, numerical simulation was used. A commercial, multi-scale and thermo-hygro dynamics analysis software, Durability of COncrete Model (DuCOM),^{28,29} is used to model water absorption and is thereafter applied in the porosity estimation and pore size distribution of the samples preconditioned to equilibrium moisture. DuCOM is capable of predicting the hydration of cement and its densification by continuous hydration of the unhydrated cement particles.^{28,29} The hydration of cement particles and moisture transport are inherently coupled during microstructure development and pore structure formation.²⁹ DuCOM applies the computational prediction of the pore structure of the matrix as a basis for moisture transport computation. Each capillary and gel porosity distribution, $\phi_{cp}(r)$ and $\phi_{gl}(r)$, is represented as

$$V = 1 - \exp(-Br), dV = Br \exp(-Br) d \ln r \quad (1)$$

where V is the fractional pore volume of the distribution up to pore radius r ; and B is the peak distribution in a logarithmic scale of the sole porosity distribution parameter.

The overall microstructure is represented as a bimodal porosity distribution through the combination of the inner and outer product contribution to the total porosity function $\phi(r)$ as

$$\phi(r) = \phi_l + \phi_g(1 - \exp(-B_g r)) + \phi_{cp}(1 - \exp(-B_{cp} r)) \quad (2)$$

where B_{gl} and B_{cp} correspond, respectively, to the gel and capillary porosity components.

Boundary conditions for water movement in DuCOM—To establish effective modeling, appropriate meshing and boundary conditions in numerical simulation are necessary. In this research, at first, one-dimensional (1-D) dominant water movement was simulated and validated by experimental results for calibrating appropriate boundary conditions. One-dimensional water sorptivity results from cylindrical samples ($\phi 100 \times 200$ mm) were used to determine appropriate boundary conditions for water movement during absorption by simulation. The measurements were conducted based on JSCE-G 582.⁶ Twenty-five mm (0.984 in.) surface zone from the bottom of the specimen was removed and the final test sample was $\phi 100$ mm \times 175 mm ($\phi 3.937 \times 8.890$ in.). Second, three-dimensional (3-D) water movement by SWAT—that is, the water penetration depth at 10 minutes of absorption, which cannot be measured experimentally—was simulated using the established and validated meshing and boundary conditions from the 1-D dominant water movement results. In the DuCOM system, a magnification factor is applied (especially in short-time water movement) for the vapor transfer coefficient. Based on the parametric investigations for the surface water absorption, four times the magnification factor of the vapor transfer coefficient for RH = 99.99% is selected to account for the transference of condensed water from the surface to the concrete.

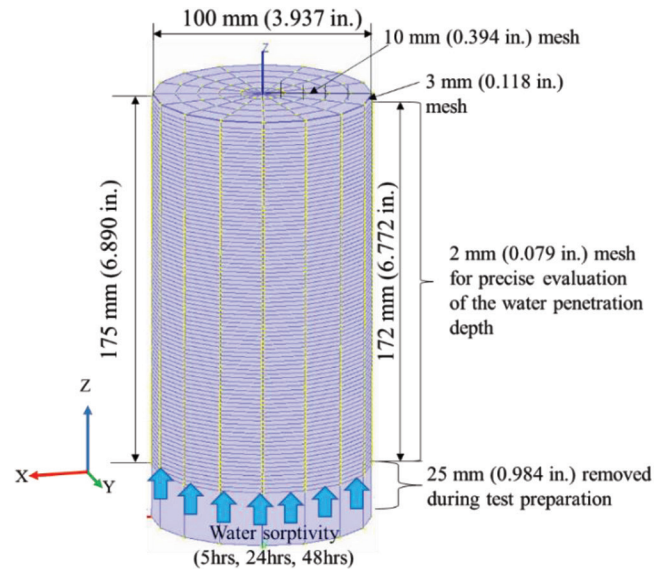


Fig. 6—Model of JSCE-G 582 test specimen.

Three types of concrete prepared with OPC and slag cement (JIS Type B slag cement) were used. The amount of water (kg/m^3 [lb/ft^3]) for mixing was kept constant at 160 kg/m^3 (9.988 lb/ft^3) for all the concrete types. Two different w/c contents (40 and 50%) for the OPC concretes were obtained by varying the amount of cement. The curing type was sealing in the mold for 28 days. The specimens were named N40-28D for OPC + 40% w/c , N50-28D for OPC + 50% w/c , and BB50-28D for slag cement + 50% w/c . The concrete mixture proportions are:

- N40-28D – sand/aggregate ratio = 45%, cement = 400 kg/m^3 (24.971 lb/ft^3), fine aggregate = 796 kg/m^3 (49.693 lb/ft^3), coarse aggregate = 973 kg/m^3 (60.742 lb/ft^3), Ad is water-reducing admixture = 1.0, AE is air-entraining agent = 0.0015 entrained air content 5.6%.
- N50-28D – sand/aggregate ratio = 47%, cement = 320 kg/m^3 (19.977 lb/ft^3), fine aggregate = 865 kg/m^3 (54.0 lb/ft^3), coarse aggregate = 975 kg/m^3 (60.876 lb/ft^3), Ad is water-reducing admixture = 1.0, AE is air-entraining agent = 0.0015 entrained air content 4.9%.
- BB50-28D – sand/aggregate ratio = 46.7%, cement = 320 kg/m^3 (19.977 lb/ft^3), fine aggregate = 854 kg/m^3 (53.313 lb/ft^3), coarse aggregate = 975 kg/m^3 (60.867 lb/ft^3), Ad is water-reducing admixture = 0.8, AE is air-entraining agent = 0.0015 entrained air content 3.5%.

Sample preparations according to JSCE-G 582 started 60 days after casting. Details of the experimental steps, conditions, test preparations, and results are documented by the author.⁸ Figure 6 shows the meshing details of the model.

COMPARISON OF SIMULATIONS AND EXPERIMENTAL RESULTS

Water penetration depths at 5, 24, and 48 hours for BB50-28D are shown in Fig. 7(a) through (c) while the effectiveness of the boundary condition on the 5 hours of water penetration depth is shown in Fig. 7(d). The penetration depth is determined as the first point where the difference in saturation degree of pore voids before and after water

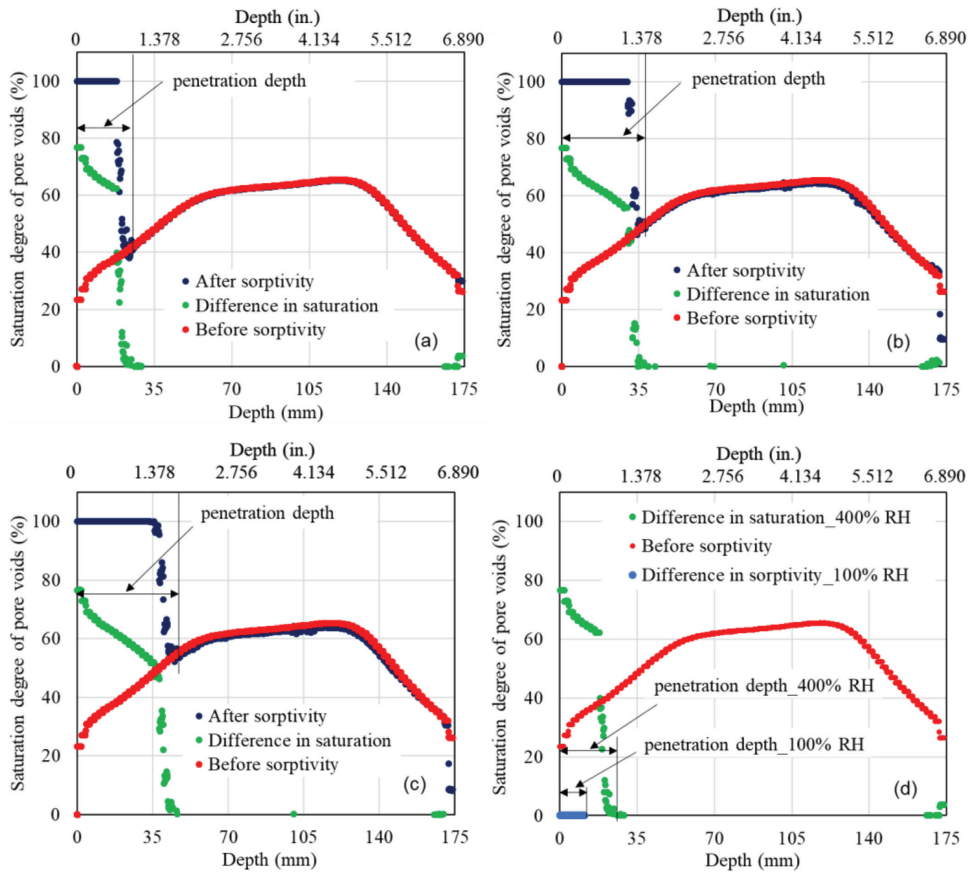


Fig. 7—Numerical modeling of water sorptivity—depth of water penetration for BB50-28D specimen: (a) 5 hours; (b) 24 hours; (c) 48 hours; and (d) effects of RH.

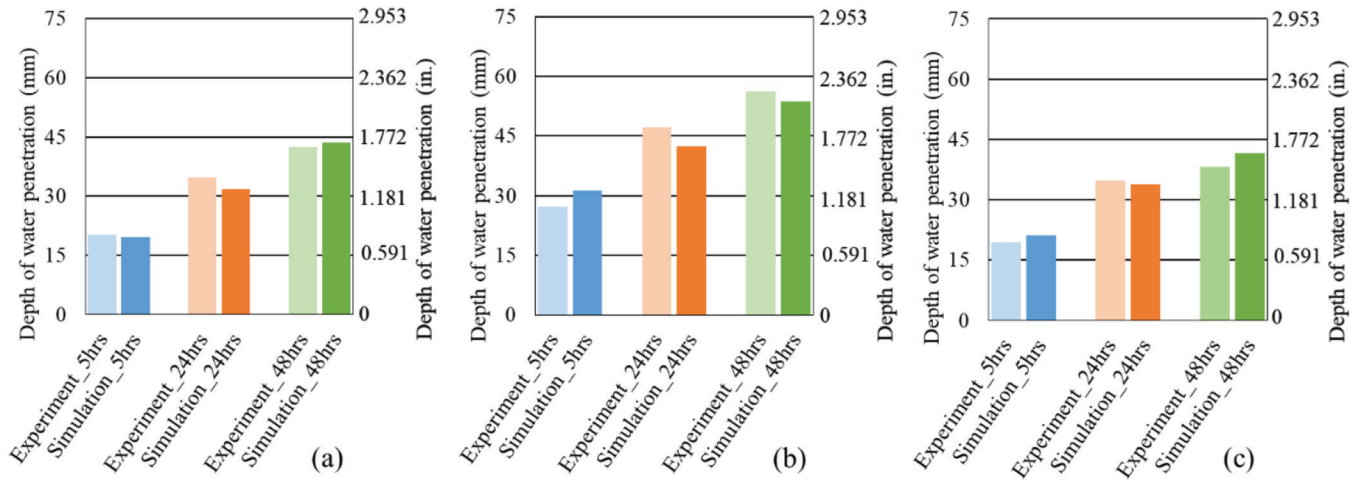


Fig. 8—Average depth of water penetration of concrete from experiment and numerical simulation: (a) N40-28D; (b) N50-28D; and (c) BB50-28D.

absorption equals zero. As for experiments, moisture penetration depth is determined by spraying a color-differentiating water detector that conforms to NDIS 3423 specifications. The measured and simulated results for the three concrete types (N40-28D, N50-28D, and BB50-28D) are compared in Fig. 8(a) through (c). A high coefficient of determination, $R^2 = 0.9438$ (Fig. 9), was obtained from the approximation of the relationship between measured and simulated results for water penetration depth by a linear function. This high

correlation validates the simulation model for evaluating water penetration depth in a 1-D dominant water movement.

The simulation model was applied to investigate the 3-D water ingress of the concrete samples (preconditioned to uniform moisture distributions and measured at several PSDs). The meshing was shown in Fig. 10 where 2 mm thick meshes were used up to 10 mm from the surface in the depth direction (z-direction) for a precise simulation of absorption amount. Also, 2 mm thick mesh sizes in the y-direction were made beyond the inner $\phi 80$ mm circle (which represents the

SWAT water cup) to evaluate the effect of 3-D water ingress. For the experiments, *CSWA* is the slope from an approximate linear regression obtained by plotting the cumulative water absorption per unit area against the square root of time (in seconds), whereas *CSWA* in the numerical simulation is deduced from the cumulative water absorption calculated by considering all the output parameters (physically adsorbed water, free water, and water fixed in hydrates) for moisture transfer in the DuCOM tool.

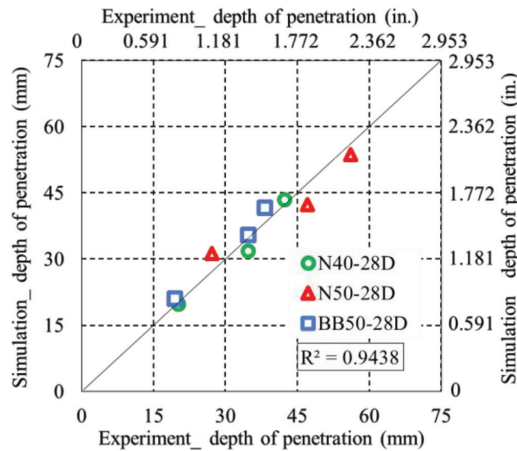


Fig. 9—Relationship between measured and simulated results for depth of water penetration.

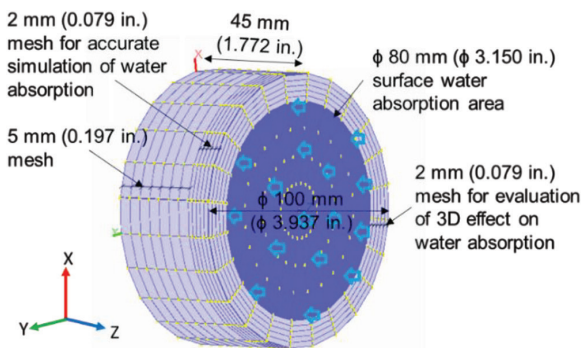
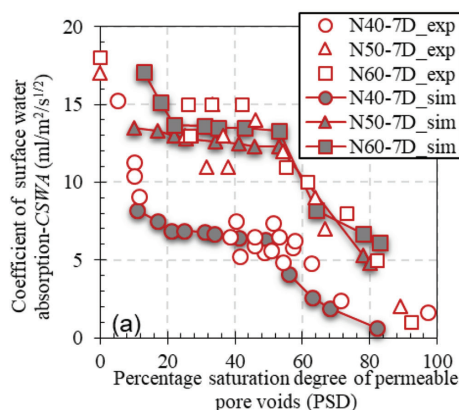


Fig. 10—Model of sample preconditioned to equilibrium moisture distribution.



RESULTS AND DISCUSSION

Influence of pore void saturation degree on water absorption for concrete with uniform moisture distribution

The effects of *PSD* on water sorptivity for the simulated and measured values are shown in Fig. 11(a) and (b). A good agreement is observed when values obtained from the simulation model are compared to the experimental results. It is seen that three regions are formed (indicated as A, B, and C) as illustrated in Fig. 12. Similar trends were seen in regions A and C. It was revealed that the water sorptivity obtained from 10 minutes of measurement exhibited a near-linear inverse relationship with *PSD* for all the samples in the two regions. From the experimental results, region A was between 0 and 20% *PSD* for all the concrete types, whereas region C was 46% *PSD* and above for N60-7D, 51% *PSD* and above for N50-7D, and 59% *PSD* and above for N40-7D. According to the increase in *PSD*, water sorptivity decreased in regions A and C. On the other hand, from simulation results, while all the concrete types revealed 0 to 20% *PSD* in region A, region C for N40-7D was 51% *PSD* and above, and region C for N50-7D and N60-7D was 54% *PSD* and above.

A different trend from regions A and C was observed in region B. From the experimental results, between 21% *PSD* and 45% *PSD*, *PSD* was seen to have almost no influence on water sorptivity for N60-7D. In the same way, the plateau zone was observed between 21% *PSD* and 50% *PSD* for N50-7D, and 21% *PSD* and 58% *PSD* for N40-7D. The simulation results showed a plateau zone at 21% *PSD* to 50% *PSD* for N40-7D, and 21% *PSD* to 53% *PSD* for N50-7D and N60-7D. Experimental results revealed that the range of region B (plateau zone) increases with a decrease in the *w/c*. This means that the volume of pore diameters related to the plateau region increases with a decrease in the *w/c* content, indicating an increase as the quality of concrete improves. The plateau region is caused by the discontinuity in the pore connections that resulted from instant rapid absorption and moisture redistribution during water absorption at region A. The discontinuous pores require a longer time for the saturation of pore voids. This is evident in Fig. 13, where the simulation results of 6 hours of surface water absorption revealed the disappearance of the plateau region. More discussion on different water absorption mechanisms that resulted in the three regions is in the subsection that follows.

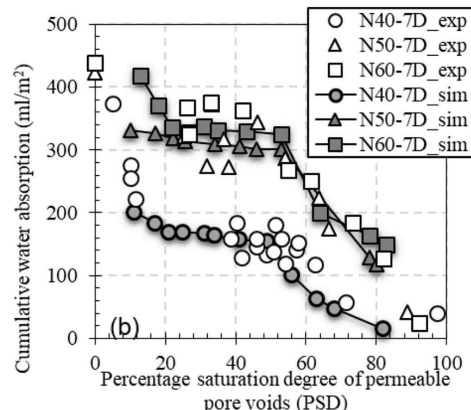


Fig. 11—Water sorptivity of concrete against PSD: (a) *CSWA* versus PSD; and (b) p_{600} versus PSD.

The estimated pore size distributions from numerical simulations are shown in Fig. 14(a). Validations of the pore size distributions obtained by the simulation tool were

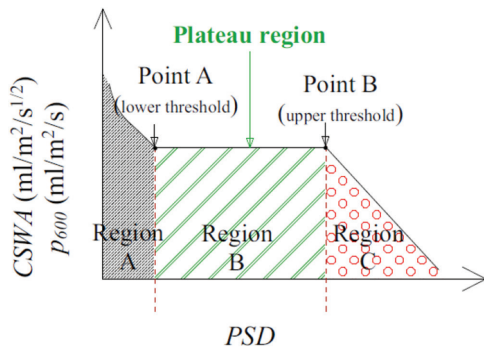


Fig. 12—Pattern diagram for relationship between sorptivity and PSD.

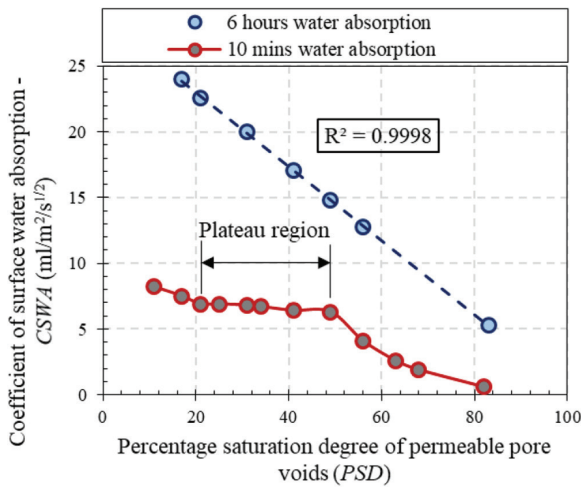


Fig. 13—Effect of long-term absorption on plateau region for N40-7D concrete by numerical simulation.

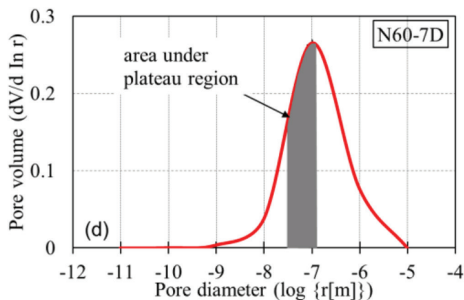
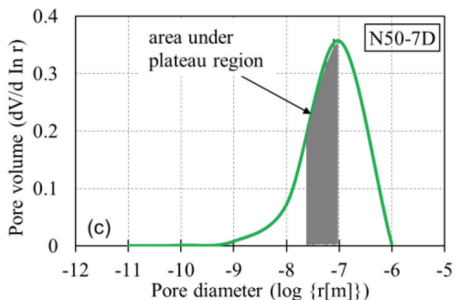
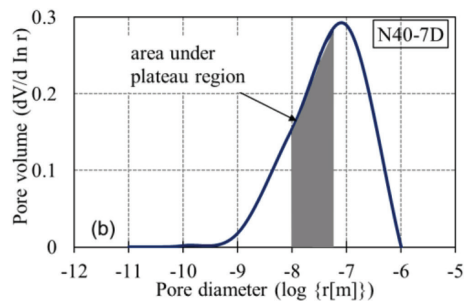
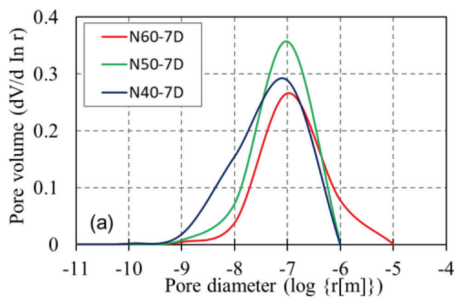


Fig. 14—Porosity estimation of pore size distribution for OPC concretes showing effective pore diameters for plateau regions from simulation: (a) pore size distribution; (b) N40-7D; (c) N50-7D; and (d) N60-7D.

not conducted as many experimental validations for many kinds of concrete have previously been documented by researchers.²⁸⁻³³ The dominant pore diameters empty for absorption and saturation during the 10 minutes of water absorption in region B (plateau region) is the shaded areas shown in Fig. 14(b), (c) and (d) for N40-7D, N50-7D, and N60-7D, respectively. It revealed that for all concrete types in this study, the maximum pore diameter corresponding to the upper limit of the plateau region is equivalent to 10^{-7} m (100 nm [3.937×10^{-3} mil, thou]). The range of dominant pore diameters differs in the three regions; thus, different water absorption mechanisms contributed to the pattern (A, B, and C regions) in the relationship between water sorptivity and PSD. In estimating the empty capillary pores available for water uptake, the saturation is taken in the order of the pore diameter starting from the smallest while neglecting ink-bottle effects because the water absorption measurements were conducted at the condition of equilibrium moisture distribution. It has been confirmed that at an equilibrium moisture distribution state only the pores of specific diameter and smaller diameter sizes are saturated; thus, the effects of the ink-bottle neck on water absorption are negligible.¹²

Absorption mechanism for water movement in regions A and C—In region A (predominately 0 to 20% PSD), which could be seen as an extremely dry region, the pore system is empty; thus, rapid surface water absorption occurs when concrete is placed in contact with water. Because the bigger gel pores are not filled, as water enters the large capillary pores, instant-rapid-partial redistribution into the smaller empty pores occurs allowing for an increase in internal swelling that reduces the pore connectivity, lowering the amount of absorption. This is similar to Rucker-Gramm and Beddoe’s revelation on the influence of gel pore water in the transport of water in much larger capillaries.¹² For this reason, surface water absorption in this region has a

near-linear inverse relationship with the saturation degree of permeable pore voids until the critical pore diameters that aid in the instant moisture redistribution are filled up. The critical pore diameter is seemingly within 20% PSD and below.³⁴

Region C, which could be seen as a wet region, similarly shows a water absorption relationship with PSD as a near-linear inverse relation. In this region, only big capillary pores that have sole water absorbency¹⁶ are empty. As absorption proceeds, smaller pores are filled, reducing the volume of the available empty pores for absorption.

Absorption mechanism for water movement in region B (the plateau region)—Nearly zero influence of PSD on water absorption is observed in this region; thus, a plateau in the pattern diagram exists. Here, the critical pore diameters that contribute to the instant-rapid-partial redistribution of moisture have already been filled. The pore diameters in this region do not directly contribute to water absorption. Capillary water absorption in this region requires a longer time (as shown in Fig. 13) for saturation of the pores due to the presence of noncontinuous finer capillary pores, less connectivity, and discontinuity in the pore system, together with the tortuous property of concrete. Because SWAT is measured only at 10 minutes, the saturation of the pores could not be attained. As seen in Fig. 14(b) through (d), the empty capillary pore diameters in this region are between 10^{-8} m (10 nm [3.937×10^{-4} mil, thou]) and 10^{-7} m (100 nm [3.937×10^{-3} mil, thou]). The pore diameters could have strong relations with the threshold pore size by the mercury intrusion porosimetry (MIP) test. When short-time water absorption measurements such as SWAT are conducted in this PSD region (plateau zone), it assesses the continuity and connectivity of the pore systems, which is the major indicator of the durability of concrete.

The threshold for the saturation degree of permeable pore voids for effective evaluation of surface water absorption is the plateau region because nearly zero effects of moisture were observed and every concrete quality was distinct. Where the quality of the mixture proportion of concrete is unknown, the upper threshold PSD, which is the most important, could be taken as “210 counts” of surface moisture meter equivalent to 58% PSD. The general water absorption mechanism, including the formation of the plateau, is represented in the schematic diagram shown in Fig. 15.

Influence of pore void saturation degree on water absorption for concrete with moisture gradient

In actual concrete structures, moisture condition inside concrete is not uniform. In many cases, there is a moisture gradient from the surface of concrete into the depth direction. Here, the effects of PSD with moisture gradient on water absorption are investigated.

The effects of surface PSD on water sorptivity were investigated using concrete blocks with internal moisture gradients. Moisture distribution in the concrete blocks exposed to 60, 80, and 99% RH was measured with embedded sensors at several depths. The count values by the moisture meter (as explained in Fig. 3) are shown in Fig. 16. The N40, N50, N60, and BB50 concretes are shown in Fig. 16(a), (b), (c),

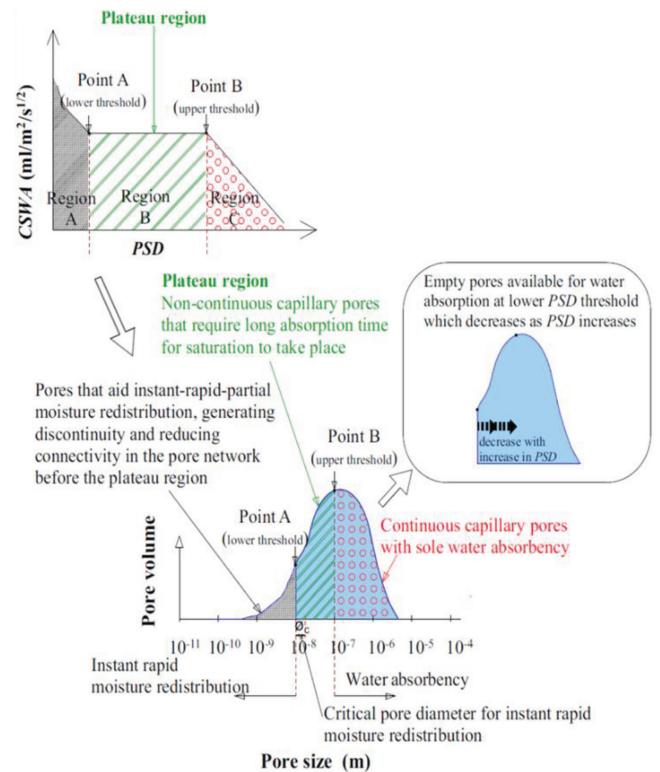


Fig. 15—Schematic diagram of water absorption mechanism for formation of plateau zone.

and (d), respectively, which are typical to different internal moisture gradients in real concrete structures.

Simultaneous measurements for surface PSD and water sorptivity are conducted with the recordings of the internal moisture gradient. The plotting of CSWA against moisture meter count values is shown in Fig. 17. Figure 17(a) shows the results for the 10D series of the concrete blocks, whereas Fig. 17(b) is for the 10W series. In Fig. 17, hollow circles represent surface PSD above the threshold whereas solid circles represent surface PSD within the threshold (plateau region) as per the upper threshold defined by 210 count value of the moisture meter.

In general, the results strongly revealed that below the 210 count value, surface PSD has almost no effect on water sorptivity for in-place concrete. Clear, acceptable grading and covercrete quality variations are seen among the eight different concrete types. It revealed visible influences of cement type, w/b content, and curing conditions on the plateau range, as well as the water sorptivity results. For all the 10D series, a near-linear inverse relation is seen above 210 count values. For some 10W series, the plateau range extended beyond 210 count values, indicating better quality of concrete with a larger volume of pores within 10 to 100 nm (3.937×10^{-4} to 3.937×10^{-3} mil, thou) diameters. It confirmed the different ranges of the plateau region observed in experiments for the preconditioned OPC samples. Where information on the w/b and curing condition of in-place concrete is available, the upper threshold PSD value could appropriately be adjusted and considered before SWAT measurement. This validates the acceptability of the proposed assessment method using an upper-threshold PSD as the maximum surface moisture content for effective

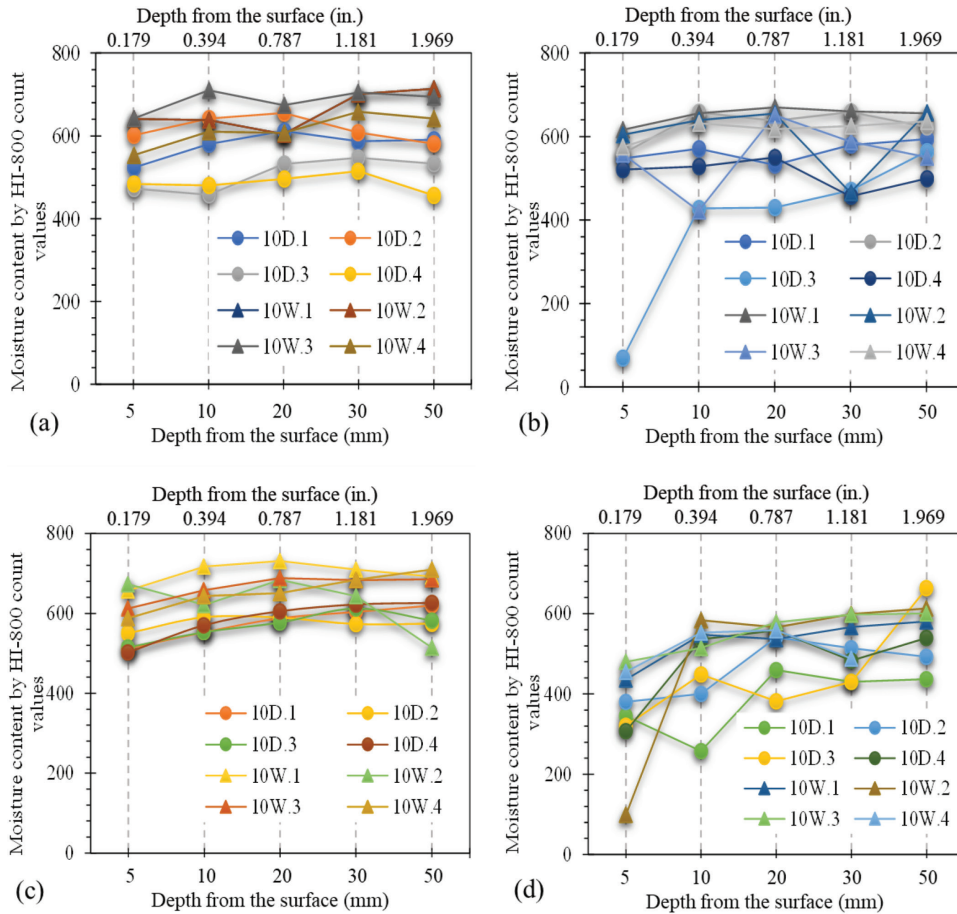


Fig. 16—Typical internal moisture distribution of concrete blocks exposed to different RH.

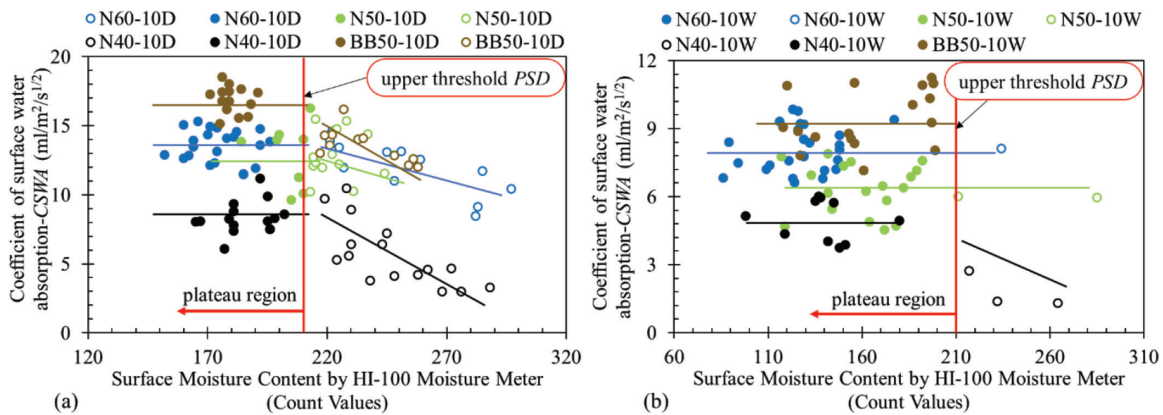


Fig. 17—Coefficient of surface water absorption—CSWA versus surface moisture content by HI-100 count values: (a) 10D series; and (b) 10W series.

durability assessment of in-place concrete structures when measuring the resistance to water ingress.

CONCLUSIONS

This study investigated the effect of saturation degree in concrete pore voids on water sorptivity, with quantitative and a clear correlation, showing the region where the degree of saturation of pore voids has almost no effect on the water resistance measurement results by the surface water absorption test. The conclusions derived from this study can be summarized as follows:

1. The initial pore void saturation degree at the cover zone of concrete for effective evaluation of the resistance to water absorption during durability assessment of in-place concrete structures was proposed based on the region where the degree of saturation has almost no effect on the measured results. Ordinary portland cement (OPC) 40, 50, and 60% water-cement ratio (w/c) concrete specimens preconditioned to uniform moisture distribution showed almost no effect of the saturation degree of permeable pore voids (PSD) on coefficient of surface water absorption ($CSWA$) within a particular PSD region (plateau region) for both the measured and simulated results. Moreover, the water sorp-

tivity of OPC and BB concrete blocks with internal moisture gradients confirmed the existence of the plateau region within the same PSD region for various patterns of internal moisture gradients.

2. When a short-term resistance to water absorption test is conducted with an initial surface moisture content within the plateau region, the measurement estimates the volume of noncontinuous finer capillary pores and evaluates the continuity and connectivity of the pore system. Continuity and connectivity of the pore system are known as the major indicator of the durability of concrete. The effective pore diameter relevant to the plateau zone is 10 to 100 nm (3.937×10^{-4} to 3.937×10^{-3} mil, thou). Measurement at this region eliminates the effects of initial surface moisture content on the measured properties.

3. To ensure the evaluation of resistance to water absorption at the noncontinuous finer capillary pore void saturation degree, the upper threshold for initial surface moisture content of concrete could be appropriately considered as equivalent to the “210 counts” of the surface moisture meter. This is the least value of the upper threshold and could be applied when information about the in-place concrete structure (such as *w/c* content and curing condition) is unknown. Where this information is available, the upper threshold may be appropriately adjusted upwards.

AUTHOR BIO

Uwazuruonye Raphael Nnodim is a Postdoctoral Researcher at the Concrete Laboratory, Civil Engineering Department, Institute of Urban Innovation of Yokohama National University, Yokohama, Japan. He received his bachelor's degree from Federal Polytechnic Nekede Owerri, Nekede, Nigeria; his PGD from National Centre for Technology Management, Ife, Nigeria; and his MPhil and PhD from Yokohama National University. He is a World Bank Scholar and a one-time recipient of the prestigious MEXT scholarship. His research interests include nondestructive durability assessment of concrete structures.

ACKNOWLEDGMENTS

This research was partly funded by the technology research and development system of The Committee on Advanced Road Technology established by the Ministry of Land, Infrastructure, Transport and Tourism (MLIT), Japan, as “Research development on quality and durability attainment system for concrete structures in various regions utilizing curing techniques and admixtures”, the commissioned research of the National Institute for Land and Infrastructure Management.

NOTATION

B	=	peak distribution in logarithmic scale of sole porosity distribution parameter
B_{cp}	=	capillary porosity component
B_{gl}	=	gel porosity component
C_{SWA}	=	coefficient of surface water absorption
DuCOM	=	Durability of Concrete Model simulation tool
PSD	=	percentage saturation degree of permeable pore voids of concrete
r	=	pore radius
SWAT	=	surface water absorption test
V	=	fractional pore volume of the distribution up to pore radius r
ϕ_{cp}	=	capillary porosity function
ϕ_{gl}	=	gel porosity function
ϕ_{lr}	=	interlayer porosity function

REFERENCES

1. Ueda, H.; Sakai, Y.; Kinomura, K.; Watanabe, K.; Ishida, T.; and Kishi, T., “Durability Design Method Considering Reinforcement Corrosion due to Water Penetration,” *Journal of Advanced Concrete Technology*, V. 18, No. 1, 2020, pp. 27-38. doi: 10.3151/jact.18.27

2. Claisse, A. P., *Transport Properties of Concrete: Measurements and Applications*, Elsevier, Amsterdam, The Netherlands, 2014.

3. Long, A. E.; Henderson, G. D.; and Montgomery, F. R., “Why Assess the Properties of Near-surface Concrete?” *Construction and Building Materials*, V. 15, No. 2-3, 2001, pp. 65-79. doi: 10.1016/S0950-0618(00)00056-8

4. ASTM C1585-04, “Standard Test Method for Measurement of Rate of Absorption of Water by Hydraulic-Cement Concretes,” ASTM International, West Conshohocken, PA, 2007.

5. BS 1881, Part 207, “Testing Concrete – Recommendations for the Assessment of Concrete Strength by Near-to-Surface Tests,” British Standards Institution, London, UK, 1992.

6. JSCE-G 582, “Test Method for Water Penetration Rate Coefficient of Concrete Subjected to Water in Short-Term,” Japan Society of Civil Engineers, Tokyo, Japan, 2018. (in Japanese)

7. Nakarai, K.; Shitama, K.; Nishio, S.; Sakai, Y.; Ueda, H.; and Kishi, T., “Long-Term Permeability Measurements on Site-Cast Concrete Box Culverts,” *Construction and Building Materials*, V. 198, No. 8, 2019, pp. 777-785. doi: 10.1016/j.conbuildmat.2018.11.263

8. Uwazuruonye, R. N., and Hosoda, A., “Investigation on Correlation between Surface Water Absorption Test and JSCE Sorptivity Test,” *Proceedings of JCI*, V. 42, No. 1, 2020, pp. 1726-1731.

9. Castro, J.; Bentz, D.; and Weiss, J., “Effect of Sample Conditioning on the Water Absorption of Concrete,” *Cement and Concrete Composites*, V. 33, No. 8, 2011, pp. 805-813. doi: 10.1016/j.cemconcomp.2011.05.007

10. Gummerson, R. J.; Hall, C.; and Hoff, W. D., “Water Movement in Porous Building Materials—II. Hydraulic Suction and Sorptivity of Brick and Other Masonry Materials,” *Building and Environment*, V. 15, No. 2, 1980, pp. 101-108. doi: 10.1016/0360-1323(80)90015-3

11. Hall, C., “Water Sorptivity of Mortars and Concretes: A Review,” *Magazine of Concrete Research*, V. 41, No. 147, 1989, pp. 51-61. doi: 10.1680/mac.1989.41.147.51

12. Rucker-Gramm, P., and Beddoe, R. E., “Effect of Moisture Content of Concrete on Water Uptake,” *Cement and Concrete Research*, V. 40, No. 1, 2010, pp. 102-108. doi: 10.1016/j.cemconres.2009.09.001

13. Sakai, Y.; Yokoyama, Y.; and Kishi, T., “Relationship Among the Permeation Rate of Water into Concrete, the Mix Design, Curing, and the Degree of Drying,” *Journal of Advanced Concrete Technology*, V. 15, No. 10, 2017, pp. 595-602. doi: 10.3151/jact.15.595

14. Parrott, L. J., “Water Absorption in Cover Concrete,” *Materials and Structures*, V. 25, No. 5, 1992, pp. 284-292. doi: 10.1007/BF02472669

15. Maruyama, I., “Multi-Scale Review for Possible Mechanisms of Natural Frequency Change of Reinforced Concrete Structures under an Ordinary Drying Condition,” *Journal of Advanced Concrete Technology*, V. 14, No. 11, 2016, pp. 691-705. doi: 10.3151/jact.14.691

16. Yokoyama, Y.; Yokoi, T.; and Ihara, J., “The Effects of Pore Size Distribution and Working Techniques on the Absorption and Water Content of Concrete Floor Slab Surfaces,” *Construction and Building Materials*, V. 50, 2014, pp. 560-566. doi: 10.1016/j.conbuildmat.2013.10.013

17. Shirakawa, T.; Shimazoe, Y.; Aso, M.; Nagamatsu, S.; and Sato, Y., “Relationship between Degree of Drying and Gas Diffusion Coefficient in Hardened Cement,” *Transactions of AIJ*, V. 64, No. 524, 1999. pp. 7-12. doi:10.3130/aifs.64.7_410.3130/aifs.64.7_4

18. Dias, W. P. S., “Reduction of Concrete Sorptivity with Age through Carbonation,” *Cement and Concrete Research*, V. 30, No. 8, 2000, pp. 1255-1261. doi: 10.1016/S0008-8846(00)00311-2

19. Dias, W. P. S., “Influence of Drying on Concrete Sorptivity,” *Magazine of Concrete Research*, V. 56, No. 9, 2004, pp. 537-543. doi: 10.1680/mac.2004.56.9.537

20. Uwazuruonye, R. N., and Hosoda, A., “Investigation of the Effects of Saturation Degree of Permeable Pore Voids for Appropriate Concrete Quality Evaluation by SWAT,” *Internet Journal of Society for Social Management Systems*, V. 12, No. 2, 2020, pp. 87-96.

21. Hayashi, K.; Akmal, U.; and Hosoda, A., “Analysis of Moisture Transfer in Surface Water Absorption Test of Concrete using Embedded Sensors,” *Proceedings of JCI*, V. 35, No. 1, 2013, pp. 1791-1794. (in Japanese)

22. Komatsu, S.; Tajima, R.; and Hosoda, A., “Proposal of Quality Evaluation Method for Upper Surface of Concrete Slab with Surface Water Absorption Test,” *Concrete Research and Technology*, V. 29, 2018, pp. 33-40. doi: 10.3151/crt.29.33

23. Hayashi, K., and Hosoda, A., “Development of Surface Water Absorption Test Applicable to Actual Structures,” *Proceedings of JCI*, V. 33, No. 1, 2011, pp. 1769-1774. (in Japanese)

24. Hayashi, K., and Hosoda, A., “Fundamental Study on Evaluation Method of Covercrete Quality of Concrete Structures by Surface Water Absorption Test,” *Journal of Japan Society of Civil Engineers, Ser. E2, Materials and Concrete Structures*, V. 69, No. 1, 2013, pp. 82-97. (in Japanese)

25. Nam, H. P., and Hosoda, A., "Improvement of Water and Chloride Penetration Resistance of Slag Concrete by Using High Alite Cement," *Proceedings of JCI*, V. 37, No. 1, 2015, pp. 661-666.

26. Ngo, V. T.; Hosoda, A.; Komatsu, S.; and Ikawa, N., "Effect of Moisture Content on Surface Water Absorption Test and Air Permeability Test," *Proceedings of JCI*, V. 40, No. 1, 2018, pp. 1725-1730

27. Hosoda, A., and Hayashi, K., "Evaluation of Covercrete Quality of Concrete Structures by Surface Water Absorption Test," *Proceedings of the IOS2016 Symposium*, 2016.

28. Maekawa, K.; Chaube, T.; and Kishi, T., *Modelling of Concrete Performance: Hydration Microstructure Formation and Mass Transport*, Spon Press, London, UK, 1999.

29. Maekawa, K.; Ishida, T.; and Kishi, T., *Multi-Scale Modeling of Structural Concrete*, Taylor & Francis, London, UK, 2009.

30. Ishida, T.; Maekawa, K.; and Kishi, T., "Enhanced Modeling of Moisture Equilibrium and Transport in Cementitious Materials under Arbitrary Temperature and Relative Humidity History," *Cement and Concrete Research*, V. 37, No. 4, 2007, pp. 565-578. doi: 10.1016/j.cemconres.2006.11.015

31. Maekawa, K.; Pimanmas, A.; and Okamura, H., *Nonlinear Mechanics of Reinforced Concrete*, Spon Press, London, UK, 2003.

32. Nakarai, K.; Ishida, T.; Kishi, T.; and Maekawa, K., "Enhanced Modeling of Microstructure Formation of Cement Hydrates Coupled with Thermodynamics," *Proceedings of Monte Verità*, Switzerland, 2005, 6 pp.

33. Nakarai, K.; Ishida, T.; Kishi, T.; and Maekawa, K., "Enhanced Thermodynamic Analysis Coupled with Temperature-dependent Microstructures of Cement Hydrates," *Cement and Concrete Research*, V. 37, No. 2, 2007, pp. 139-150. doi: 10.1016/j.cemconres.2006.10.006

34. Uwazuruonye, R. N., "Effects of Pore Void Saturation Degree on Nondestructive Tests for Durability Assessment of Concrete Structures," PhD thesis, Yokohama National University, Yokohama, Japan, 2020, 155 pp. doi: 10.18880/00013481

APPENDIX A

Figure A1 shows the detailed geometry of the SWAT device, while Table A1 shows the conventional grading of covercrete quality by SWAT.

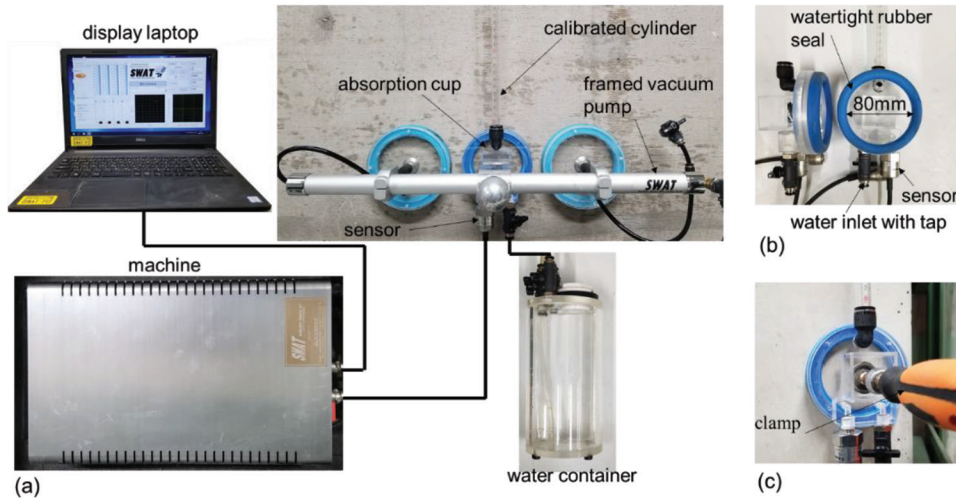


Fig. A1—Detailed geometry of SWAT device: (a) system; (b) details of absorption cup; and (c) detail of attachment onto small specimen.

Table A1—Grading of covercrete quality by SWAT

Water absorption rate at 10 minutes (600 seconds)	Quality		
	Good	Ordinary	Poor
p_{600} , mL/m ² /s	<0.25	0.25 to 0.50	>0.50